RSC Advances

This is an *Accepted Manuscript*, which has been through the Royal Society of Chemistry peer review process and has been accepted for publication.

Accepted Manuscripts are published online shortly after acceptance, before technical editing, formatting and proof reading. Using this free service, authors can make their results available to the community, in citable form, before we publish the edited article. This *Accepted Manuscript* will be replaced by the edited, formatted and paginated article as soon as this is available.

You can find more information about *Accepted Manuscripts* in the Information for Authors.

Please note that technical editing may introduce minor changes to the text and/or graphics, which may alter content. The journal's standard Terms & Conditions and the Ethical guidelines still apply. In no event shall the Royal Society of Chemistry be held responsible for any errors or omissions in this *Accepted Manuscript* or any consequences arising from the use of any information it contains.

ROYAL SOCIETY OF CHEMISTRY

www.rsc.org/advances

Please do not adjust margins

Journal Name

COMMUNICATION

Facile preparation of highly electrically conductive films of silver nanoparticles finely dispersed in polyisobutylene-*b*-poly(oxyethylene)-*b*-polyisobutylene triblock copolymers and graphene oxide hybrid surfactants

Received 00th January 20xx,
Accepted 00th January 20xx

DOI: 10.1039/x0xx00000x

www.rsc.org/

Chih-Wei Chiu* and Gang-Bo Ou

We report the development of a facile method for the preparation of highly electrically conductive silver nanoparticle (AgNP) films finely dispersed in novel organic/inorganic nanohybrid surfactants consisting of an amphiphilic polymeric dispersant and graphene oxide. The production of AgNPs with a narrow size distribution and a 20 nm diameter was observed by transmission electron microscopy. Moreover, a hybrid film exhibiting a low sheet resistance of 5.2×10^{-2} Ω/sq was prepared by controlling the heat treatment of the AgNPs sample. The resulting highly electrically conductive films have great potential for application in electrically conducting devices.

Introduction

Graphene, a 2-D carbon-based material, is formed from layered exfoliated graphite structures, which are composed of a planar honeycomb arrangement containing sp^2 hybridized aromatic carbon atoms. Graphene was first discovered by Andre Geim and Konstantin Novoselov in 2004.[1,2] It has been reported that graphene possesses excellent physical properties such as high electronic conductivity,[3–5] thermal conductivity,[6–8] and mechanical properties.[9–11] Recently, graphene has been developed for use in a range of applications, including electronic devices,[12] thermal solutions,[13] chemical catalysts,[14] biosensors,[15] and hybrid composites.[16,17] Generally, graphene is incompatible with organic polymers due to its inherent tendency to agglomerate in polymer matrices and organic media.[18] Common approaches for preparing organically modified graphene include the following methods: 1) Covalent grafting to the graphene surface;[19] and 2) Use of noncovalent bonding interactions such as π–π stacking, lone pair-π interactions, hydrophobic effect, and hydrogen bonding.[20] In order to maintain a homogenous suspension, and in particular a nanoscale dispersion, a suitable stabilizing agent is often required.[21,22]

Silver nanoparticles (AgNPs) are widely used in a variety of devices and applications.[23] However, the majority of synthetic methods do not impart long-term stability to AgNPs.[24] In general, common organic surfactants or amphiphilic polymers are employed for stabilizing the resulting AgNPs. In addition to their stabilizing effects, organic surfactants may act as templates for tailoring AgNPs into a spherical structure.[25] AgNPs have also been reported to exhibit unique properties, allowing their application as conducting materials,[26] catalysts,[27] and biosensors.[28] More specifically, in terms of the recent development of electronic devices, to decrease the thickness of films along with the width of printed loops, the synthesis of AgNPs in different forms (e.g., as a conductive paste) is required.[29] The preparation of coated silver films with a low sheet resistance of 10^{-1} Ω/sq is difficult with the existing technology due to unstable preparation processes.[30,31] Recently, the synthesis of AgNPs in the presence of inorganic stabilizers such as SiO_2,[32] TiO_2,[33] Al_2O_3,[34] carbon black,[35] CNTs,[36] graphene,[37] and nanoclay[38] has been demonstrated to be advantageous for avoiding organic components. The use of inorganic stabilizers to support surface interactions with both Ag^+ and the generated Ag^0 could result in solution stability for fine particles. In the organic-free system, naked AgNPs are unique in that they exhibited low-temperature melting.[39] The plate-like graphene oxide and, in particular, the exfoliated nanosheets containing a high aspect ratio, may therefore provide a high surface area for interaction with AgNPs.

We herein report the facile preparation of highly electrically conductive AgNP films by anchoring novel organic/inorganic nanohybrid surfactants with a polymeric dispersant and graphene oxide (GO). The organic dispersant, a polyisobutylene-*b*-poly(oxyethylene)-*b*-polyisobutylene (PIB-POE-PIB) triblock copolymer, was synthesized from polyisobutylene-*g*-succinic anhydride (PIB-SA) and

Department of Materials Science and Engineering, National Taiwan University of Science and Technology, Taipei 10607, Taiwan
**Corresponding author: Tel: +886-2-2737-6521; Fax: +886-2-2737-6544; E-mail: cwchiu@mail.ntust.edu.tw*
Electronic Supplementary Information (ESI) available: [Experimental procedures, UV-Vis spectra, TEM micrographs, FE-SEM micrographs, and EDS analysis of the AgNP/PIB-POE-PIB/GO nanohybrids are available in the supporting information. In addition, a movie showing a demonstration of the LED bulbs illuminated using the electrical conductivity of the nanohybrid films is provided.]. See DOI: 10.1039/x0xx00000x

RSC Advances Accepted Manuscript

Please do not adjust margins

poly(oxyethylene)-diamine (POE) of 2000 g/mol molecular weight (*M*w) through continuous amidation and imidation reactions. A high aspect ratio and surface area of GO are expected to be achieved by the chemical exfoliation of a layered graphite structure. Transmission electron microscopy was used to determine the size distribution and diameter of the synthesized AgNPs. We aim to prepare films exhibiting low sheet resistance by increasing the continuous Ag network structure through temperature control. It is expected that the resulting nanohybrid films can be used in various electrically conducting devices.

Experimental

Materials

The graphene oxide (GO) used in this study was prepared according to a modified Hummers method and was obtained from Enerage Inc., Taiwan.[40–42] The GO nanosheets were decorated with various oxygen functional groups (e.g., hydroxyl, carboxylic, and epoxide moieties) and were composed of a sheet carbon structure with variable oxygen contents of 4%, 20%, and 50% (abbreviated as GO-4%, GO-20%, and GO-50%, respectively). Silver nitrate ($AgNO_3$, purity 99.9%) was obtained from Sigma-Aldrich Chemical Co. and *N*,*N*-dimethylformamide (DMF) was obtained from TEDIA Company Inc. Polyisobutylene-*g*-succinic anhydride (PIB-SA) with a molecular weight (*M*w) of 1335 was purchased from Chevron Corp. Poly(oxyethylene)-diamine (POE-diamine), with the designated trade name of Jeffamine® ED2003 (abbreviated POE-2000), was obtained from Huntsman Chemical Co.

Synthesis of polyisobutylene-*b*-poly(oxyethylene)-*b*-polyisobutylene (PIB-POE-PIB) triblock copolymers

The PIB-POE-PIB triblock dispersant was synthesized from the reaction of PIB-SA and POE-2000 (2:1 molar ratio) according to the following procedure. A solution of PIB-SA (50.0 g, 0.038 mol) in tetrahydrofuran (THF, 200.0 g) was added to a 1000 mL three-necked, round-bottomed flask equipped with a machine stirrer and a thermocouple. A solution of POE-2000 (38.0 g, 0.019 mol) in THF (152.0 g) was then added dropwise. With continuous stirring, the mixture was held at 25 °C for 3 h. Then, the reaction mixture was analyzed by Fourier transform infrared spectroscopy (FT-IR). Characteristic absorption peaks at 1556 cm^{-1} and 1644 cm^{-1} were observed for the amido acid functionalities. When the temperature was increased to 150 °C and maintained for 3 h, major absorption peaks at 1713 cm^{-1} and 1770 cm^{-1} were observed, corresponding to the cyclized imide functionality. This indicated conversion of the linking functional group from amido acid to imide. Finally, the product was recovered by extraction with water to remove unreacted amines, followed by the removal of the organic solvent by rotary evaporation under vacuum.

Preparation of AgNP/PIB-POE-PIB/GO nanohybrids

A typical procedure for the preparation of stable AgNPs *via* an *in situ* reduction of $AgNO_3$ in the presence of the PIB-POE-PIB triblock copolymer and GO is described as follows. A suspension of GO (0.5 g GO-4% powder; 1 wt%) was dispersed by agitation in deionized water/DMF = 1:1 (50 mL) at 25 °C for 10 min, followed by the addition of a solution of PIB-POE-PIB (2.5 g) and silver nitrate (2.5 g, 0.015 mol) dissolved in deionized water/DMF = 1:1 (500 mL). To obtain the desired weight ratios of $AgNO_3$/PIB-POE-PIB/GO-4%, i.e., 5:5:1, 10:10:1, and 20:20:1, a homogenous suspension was obtained by the simple mixing of $AgNO_3$, PIB-POE-PIB, and GO-4%. These mixtures were stirred continuously for 8 h at 80 °C, and the color changes were monitored by UV-Visible (UV-Vis) spectroscopy. A color change from black to dark-yellow indicated a reduction of Ag^+ ions to Ag particles. In addition, GO with different oxygen contents was used in the AgNP dispersion according to a similar procedure. The control experiment using PIB-POE-PIB generated only a homogeneous colloidal Ag solution. UV absorption was measured using 0.1 g of solution in 3.0 g distilled water. Furthermore, all products were analyzed by TEM and FE-SEM.

Preparation of AgNP/PIB-POE-PIB/GO nanohybrid films

The conductive films were easily prepared using a casting solution method. The nanohybrid films were cast on either polyimide (PI) film (flexible substrate) or glass (rigid substrate), depending on the field of the desired application. The resulting film (2 cm × 2 cm) was first washed with 1:1 ethanol/water (×3), after which it became suitable for use as the substrate. The nanohybrid suspension (0.5 g) was then cast on a piece of film, and the film placed in a high-temperature oven and was heated at 60 °C, 250 °C, 300 °C, or 350 °C for 30 min under air. The resulting flexible and conductive films were obtained and characterized as described below.

Characterization and instruments

Fourier transform infrared spectroscopy was carried out on a Perkin-Elmer Spectrum One FT-IR Spectrometer between 4000 and 400 cm^{-1}. The 0.1 wt% PIB-POE-PIB dispersants were prepared by dissolving them in THF, followed by evaporation to obtain a thin film on a KBr plate. The AgNP solution was characterized by UV-Vis spectroscopy using a Shimadzu UV-2450 spectrophotometer. Transmission electron microscopy was performed using Zeiss EM 902A, operated at 80 kV. The sample solutions (1 wt% in deionized water/DMF = 1:1 cosolvent) were deposited onto a carbon-coated copper grid. Field emission scanning electronic microscopy was performed using Zeiss EM 902A, operated at 80 kV. The samples were prepared by dropping a small amount of the AgNP hybrids onto a clean glass surface, followed by dehydration in an oven at 80 °C for over 2 h. The samples were then fixed on an FE-SEM holder using a conductive carbon paste and coated with a thin layer of Au prior to measurement. Surface elemental analysis was carried out using energy dispersive X-ray spectroscopy (EDS, OXFORD INCA ENERGY 400). Sheet resistance measurements for the film containing AgNP were performed using a Mitsubishi MCP-T610 digital source meter equipped with a four-point probe. A demonstration of LED lamps (power dissipation = 100 mW, peak forward current = 100 mA) was designed to confirm the conductive ability of the film.

RSC Advances Accepted Manuscript

This journal is © The Royal Society of Chemistry 20xx

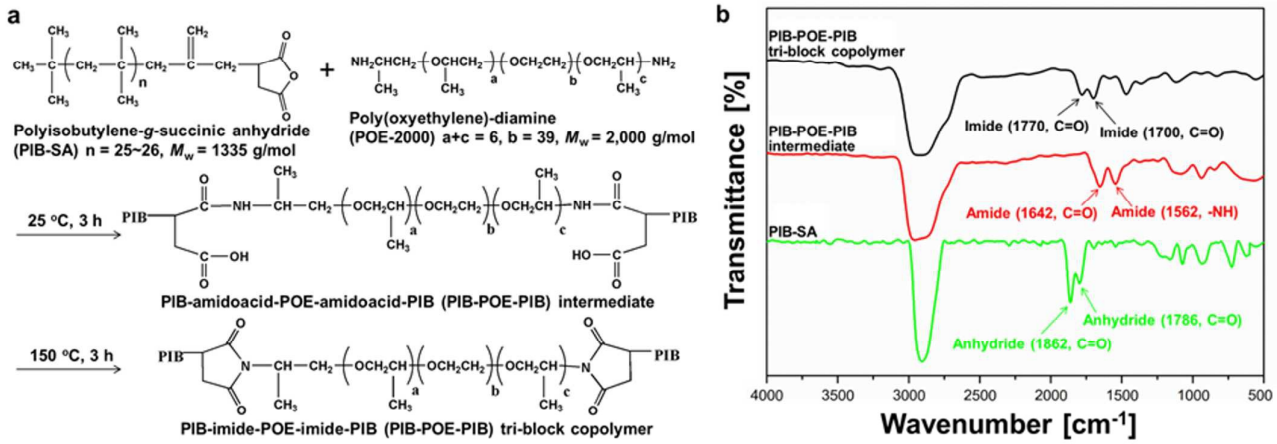

c

Sample	H_2O	EtOH	MeOH	DMF	Toluene	Decane
PIB-POE-PIB tri-block copolymer	+	+	+	+	+	+
PIB-SA	–	–	–	–	+	+
POE-2000	+	+	+	+	+–	–

+: soluble; + –: soluble but forming sediments after 2 h settlement; – : insoluble.

Fig. 1 Synthesis and characterization of polyisobutylene-*b*-poly(oxyethylene)-*b*-polyisobutylene (PIB-POE-PIB) triblock copolymers. (a) Synthesis of PIB-POE-PIB triblock structures (polymeric dispersants) from polyisobutylene-*g*-succinic anhydride (PIB-SA) and poly(oxyethylene)-diamine (POE) *via* amidation and imidation reactions. (b) FT-IR spectra of the PIB-SA, PIB-POE-PIB intermediate, and PIB-POE-PIB triblock copolymer. (c) Solubilities of PIB-SA, POE-2000, and the PIB-POE-PIB triblock copolymer.

Results and discussion

Synthesis of the PIB-POE-PIB triblock copolymer for use as an organic dispersant

Synthesis of the PIB-POE-PIB triblock copolymer involved the reaction of a cyclic anhydride ($–CCH_2(CO)_2O$) and an amine group ($–NH_2$) to produce the amido acid and imide linkage groups, as shown in **Fig. 1a**. The mechanisms of the formation of the PIB-POE-PIB intermediates and PIB-POE-PIB triblock copolymer were confirmed by FT-IR absorption measurements (**Fig. 1b**), which confirmed the presence of chemical functionalities such as the polyisobutylene-block amide and imide linking groups. To prepare the block copolymer, the ring-opening reaction of the anhydride group was first carried out at 25 °C for over 3 h, leading to complete conversion. The characteristic peaks at 1786 cm^{-1} and 1862 cm^{-1}, corresponding to the starting anhydride, disappeared during the reaction, while the peaks corresponding to the amide appeared at 1562 cm^{-1} and 1642 cm^{-1}, indicating the successful ring opening of the anhydride by the amine. The amido acid linkage then underwent a ring-closing step to afford the imide-linked PIB-imide-POE-imide-PIB at 150 °C after 3 h. The ring-closing step and formation of the imide functionalities were confirmed by the appearance of a strong imide absorption band at 1700 cm^{-1} and a weaker absorption band at 1770 cm^{-1}. In addition, **Fig. 1c** demonstrates that the solubility of the amphiphilic PIB-POE-PIB triblock copolymer in water and organic solvents was dependent on the relative ratio of the hydrophobic PIB block and the hydrophilic POE block. PIB-SA was highly hydrophobic due to the abundance of long alkyl chains. In comparison, POE-2000 was hydrophilic, being dispersible only in water and polar solvents and insoluble in nonpolar organic solvents such as toluene and decane. We found that the PIB-derived copolymer exhibited amphiphilic properties, as it is dispersible in both water and organic media. This was achieved by the addition of hydrophilic segments of POE, which altered the solubility of the copolymer. Thus, the amphiphilic or hydrophilic/hydrophobic solubility of each PIB-POE-PIB triblock copolymer could be tailored by the incorporation of different quantities of POE and PIB.

Preparation of colloidal AgNP dispersed in PIB-POE-PIB/GO nanohybrids as organic/inorganic dispersants

Due to the strong π-π stacking of the graphene surface, graphene is generally unstable in and incompatible with organic media, forming aggregates and large particles. Through ultrasonic dispersion, the graphene sheets can be finely dispersed and maintained in a homogenous state in suitable dispersants, thus expanding their possible applications. GO sheets contain various oxygen functional groups, containing oxidized edges with abundant carbonyl functionalities, and graphene surfaces decorated with epoxide and hydroxyl groups. These oxygen functional sites on the GO surface provide versatile points for chemical functionalization or

RSC Advances Accepted Manuscript

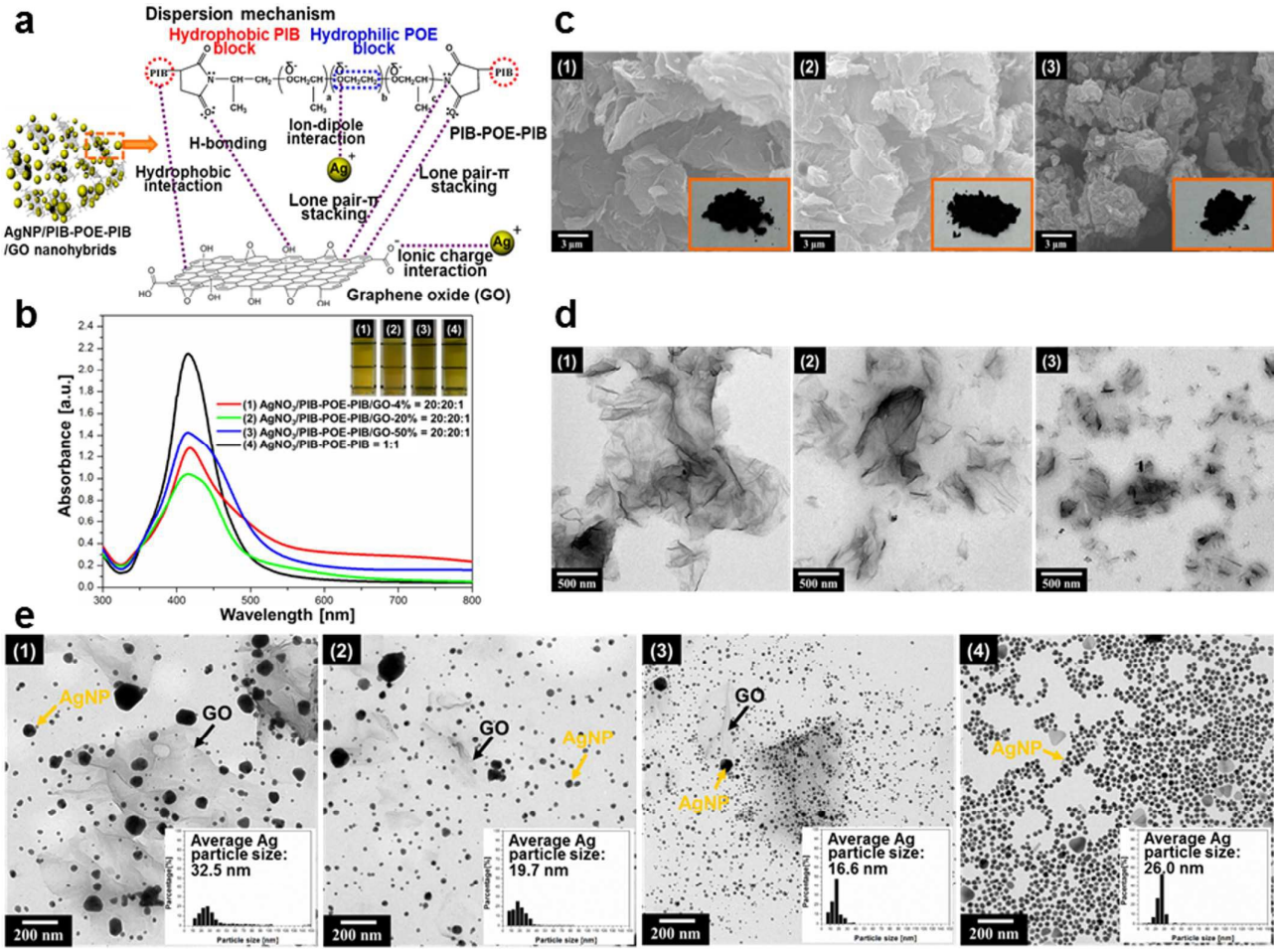

Fig. 2 Synthesis and dispersion mechanisms of AgNP/PIB-POE-PIB/GO nanohybrids. (a) Schematic illustration of AgNP/PIB-POE-PIB/GO hybrid suspensions finely dispersed through various noncovalent interactions. (b) UV-Vis absorption spectra of colloidal AgNPs in the hybrid (weight ratio = 20:20:1) containing PIB-POE-PIB and GO (oxygen contents: (1) 4%, (2) 20%, and (3) 50%). (4) $AgNO_3$/PIB-POE-PIB reduction with a weight ratio of 1:1. Inset: Yellow-gold solutions confirming AgNP formation following treatment at 80 °C for 6–8 h. (c) FE-SEM micrographs of pristine GO with oxygen contents of (1) 4%, (2) 20%, and (3) 50% (insets correspond to the raw materials of GO powder). (d) TEM micrographs of a GO/PIB-PEO-PIB solution with a 1:1 weight ratio, and GO oxygen contents of (1) 4%, (2) 20%, and (3) 50%. (e) TEM micrographs and particle size histograms based on the TEM images of colloidal AgNPs in a AgNP/PIB-POE-PIB/GO hybrid with GO oxygen contents of (1) 4%, (2) 20%, and (3) 50%. (4) $AgNO_3$/PIB-POE-PIB reduction using a 1:1 weight ratio.

noncovalent interactions, resulting in the improved compatibility of GO with organic media and in polymer composites. It is therefore necessary to design the dispersant structure for a range of GO/surfactant hybrid dispersion mechanisms, using various noncovalent approaches to fine-tune the interphase forces between GO and the surfactant. The optimal balance and dispersion performance of five types of noncovalent forces (hydrophobic interactions, hydrogen bonding, ion-dipole interactions, lone pair-π-stacking, and ionic charge interactions) between the AgNPs, PIB-POE-PIB triblock copolymer, and GO are illustrated in **Fig. 2a**. The PIB-POE-PIB dispersants have been designed to contain polar functionalities that are noncovalently tethered to GO and to the AgNPs. In addition, the GO-supporting material bears carbonyl groups on the surface, which are capable of stabilizing the AgNPs in the *in situ* reduction of silver nitrate through ionic interactions. The oxyethylene backbone lone pair of the polymeric dispersant allowed interaction with the silver ions, thus aiding in the homogeneous production of AgNPs. Through the noncovalent van der Waals forces and ionic charge interactions, AgNPs deposit on both the GO and the polymeric dispersant surfaces. Thus, the geometric differences between the two nanomaterials and the noncovalent interactions involved in the functional site of the POE $(–CH_2CH_2O–)_x$ block lead to a preparation method for AgNP/PIB-POE-PIB/GO nanohybrids, while their mutual interacting forces afford well-dispersed nanohybrid solutions.

RSC Advances Accepted Manuscript

This journal is © The Royal Society of Chemistry 20xx

Table 1. UV-Vis absorption, particle size, and sheet resistance of AgNP/PIB-POE-PIB/GO nanohybrids.

Sample	Weight ratio (w/w/w)	UV-Vis absorption (nm)	Average Ag particle size by TEM (nm)[a]	Sheet resistance (Ω/sq)[b]
AgNP/PIB-POE-PIB/GO-4%	5:5:1	421	--	1.2×10^{2}
	10:10:1	418	--	9.6×10^{0}
	20:20:1	418	32.5	9.6×10^{-1}
AgNP/PIB-POE-PIB/GO-20%	5:5:1	424	--	1.2×10^{0}
	10:10:1	421	--	5.8×10^{-1}
	20:20:1	415	19.7	1.8×10^{-1}
AgNP/PIB-POE-PIB/GO-50%	5:5:1	442	--	3.4×10^{-1}
	10:10:1	442	--	1.5×10^{-1}
	20:20:1	415	16.6	5.2×10^{-2}
AgNP/PIB-POE-PIB	1:1	416	26.0	1.8×10^{-1}

[a] Average particle sizes of silver were measured by TEM.
[b] Solution coating on a glass substrate with 60-µm-thick hybrid film at 350 °C, and the resulting sheet resistance measured using a four-point probe.

In the synthesis and dispersion of the AgNPs, DMF was commonly used as the solvent, as it also played the role of a reducing agent. Besides the good dispersion of AgNP/PIB-POE-PIB/GO hybrids in DMF/H_2O, DMF also converted Ag^+ ions into Ag particles, leading to the *in situ* preparation of AgNPs. The redox mechanism involving DMF is shown in **Scheme S1**. The AgNP/PIB-POE-PIB/GO mixtures containing different component weight ratios were subjected to the redox reaction at 80 °C, and they were then analyzed according to the solution color and by UV-Vis spectroscopy. The results from these analyses are summarized in **Fig. 2b** and **Table 1**. When the weight ratio of the AgNP/PIB-POE-PIB/GO hybrid was 20:20:1, a characteristic peak corresponding to AgNP absorbance was observed, thus confirming the generation of homogenous AgNPs. In addition, the gold-yellow color of the solution in the presence of organic PIB-POE-PIB and GO suggests the formation of AgNPs through the reduction of silver nitrate. The UV-Vis spectra indicated the presence of nanometer-scale Ag^0 particles through the characteristic peak absorption at 410–420 nm with $AgNO_3$/PIB-POE-PIB/GO weight ratios of 5:5:1, 10:10, and 20:20:1, where GO with 4%, 20%, and 50% oxygen contents was used. In a control experiment, a polymeric surfactant was used as the stabilizer instead of the PIB-POE-PIB/GO hybrids. Maintaining the $AgNO_3$/POE-imide weight ratio at 1:1 gave absorbance due to the AgNPs (*ca.* 416 nm), giving a dark-yellow solution. The characteristic peak absorption indicated red shift of the AgNPs.

The micrographs of the powder form and the suspension of GO nanosheets were then characterized by FE-SEM (**Fig. 2c**) and TEM (**Fig. 2d**). The observations with the dispersant yielded GO particles of 500–1000 nm in diameter. Good dispersion of the AgNPs on the nano-GO surfaces and polymer chains was directly observed in TEM micrographs, whilst the inset images show the size distribution based on the TEM images (**Fig. 2e** and **Fig. S1–S3**). During $AgNO_3$ reduction, the AgNPs were generated, growing in particle size while adhering to the GO sheet surface or to the polymer chain. The average size of the AgNPs decreased from 32.5 to 16.6 nm, while the size distribution narrowed with an increase in the GO nanosheet oxygen content, which provided additional interaction sites. In the control experiment, the PIB-POE-PIB dispersant alone was used as the stabilizer, giving larger AgNPs measuring approximately 26.0 nm by TEM measurements. Therefore, the differences in stability between the AgNP colloids in GO and PIB-POE-PIB can be attributed to strong interactions between the AgNPs, polymer, and sheet matrix.

Preparation of highly conductive films

After heating the nanohybrids, the thermal degradation of the organic dispersant and the hybrid was examined by thermogravimetric analysis (TGA) (**Fig. 3a**). During the measurement of the thermal degradation of the hybrids, the TGA curves indicated a two-step thermal degradation at 250 °C and 350 °C. A homogeneous hybrid suspension of AgNP/PIB-POE-PIB/GO was cast on the glass or polymer substrate and

RSC Advances Accepted Manuscript

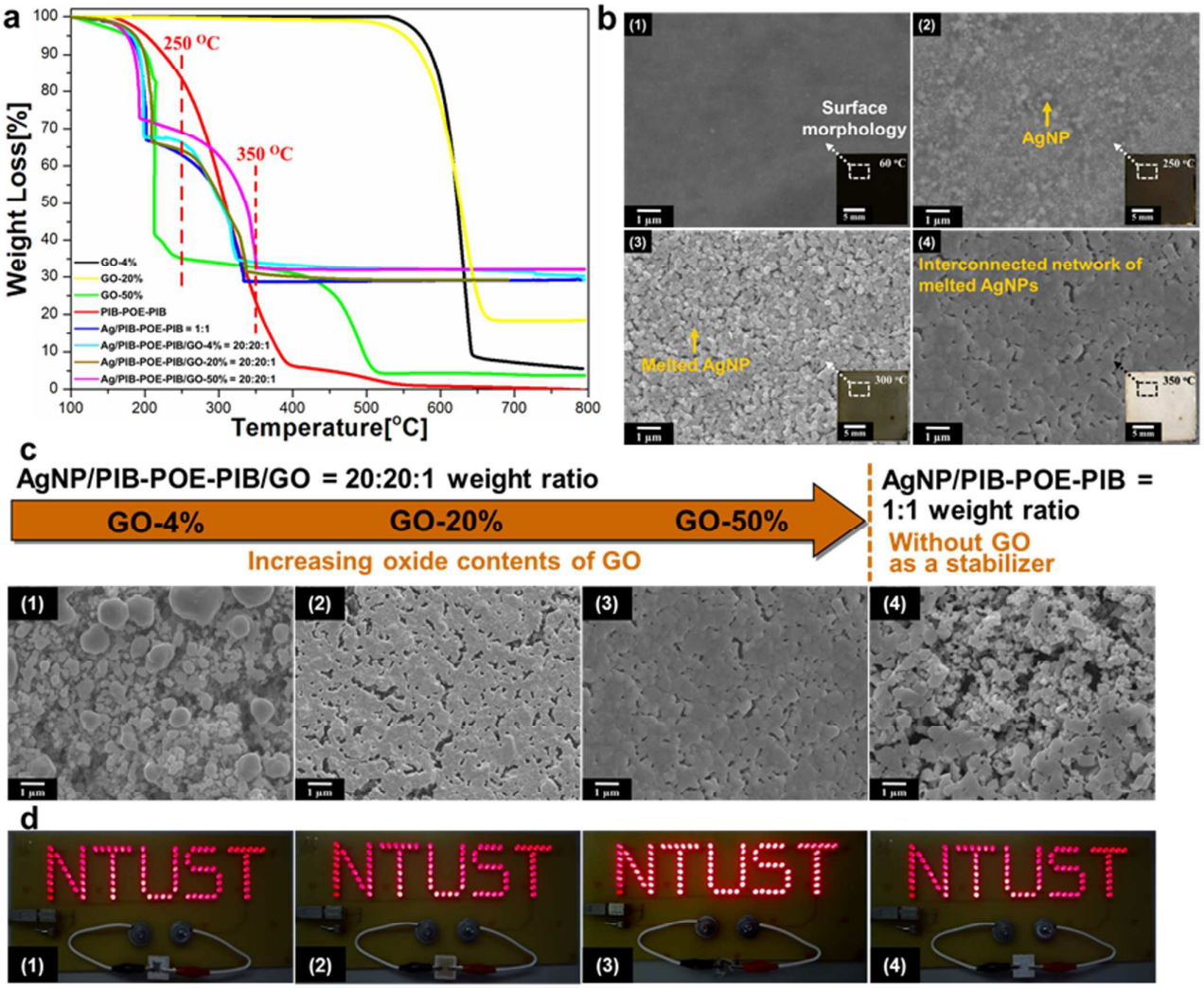

Fig. 3 Preparation of highly electrically conductive films. (a) TGA plots of AgNP/PIB-POE-PIB/GO nanohybrids with different weight fractions. (b) FE-SEM micrographs of AgNP/PIB-POE-PIB/GO nanohybrid films with a 20:20:1 weight fraction with heat treatments of (1) 60 °C, (2) 250 °C, (3) 300 °C, and (4) 350 °C for 30 min each. Insets: Photographic images of melting AgNPs on the surface of the glass substrate, used to achieve the silver-metal white color. (c) FE-SEM micrographs of AgNP/PIB-POE-PIB/GO nanohybrids with a 20:20:1 weight fraction, and with GO oxygen contents of (1) 4%, (2) 20%, and (3) 50%. (4) A $AgNO_3$/PIB-POE-PIB hybrid with a 1:1 weight fraction following 350 °C heat treatment. (d) Demonstration of conductivity based on the FE-SEM micrographs by heating AgNP/PIB-POE-PIB/GO films at 350 °C with a 20:20:1 weight fraction, and with GO oxygen contents of (1) 4%, (2) 20%, and (3) 50%. (4) A AgNP/PIB-POE-PIB hybrid with a 1:1 weight fraction.

was subjected to a series of thermal treatments. Through the heat treatment process, the AgNP/PIB-POE-PIB/GO-50% hybrid films (20:20:1 weight ratio) were prepared by using the TGA traces at a range of temperatures (60 °C, 250 °C, 300 °C, and 350 °C) over 30 min. During the solution casting preparation method, a color change from black to metal white was observed because of stepwise heating and Ag migration onto the surface of the hybrid film (**Fig. 3b**). The FE-SEM morphologies indicated the movement of AgNPs onto the GO film surface; the subsequent aggregation of silver particles into larger species forms an interconnected network structure at 350 °C. **Fig. 3c** shows the results of the heat treatment, leading to the melting of the AgNPs into larger aggregates or interconnections. In this case, the AgNP/PIB-POE-PIB/GO nanohybrids with a 20:20:1 weight ratio and GO containing 4%, 20%, and 50% oxygen were used. The AgNPs on the GO nanosheets were homogeneous in size distribution. They also possessed low surface energy and exhibited the interconnected network morphology of the melted AgNPs. In addition, elemental analyses on a AgNP/PIB-POE-PIB/GO-50% hybrid with a 20:20:1 weight ratio heated at 300 °C was carried

This journal is © The Royal Society of Chemistry 20xx

RSC Advances Accepted Manuscript

out using EDS (Supporting Information **Fig. S4**). A denser melted Ag was found on the top layer of the film formed through complete degradation of the organic component in the heat treatment. Furthermore, it was demonstrated that the difference in sheet resistance could be used to illuminate light-emitting diodes (LED), as shown in **Fig. 3d**, **Fig. S5**, and **Movie S1**. When the AgNP/PIB-POE-PIB/GO-50% hybrid with a weight ratio of 20:20:1 was heated at 350 °C, the surface resistance was found to be sufficiently low to illuminate the LED lamps. In contrast, the surface resistance of the AgNP/POE-imide hybrid film was higher, and was thus less effective in illuminating the LED bulbs.

The electrical conductivity of the nanohybrid films was examined as a function of AgNP content and heat treatment, as shown in **Tables 1**, **S1**, and **S2**. When the hybrid materials were subjected to heat treatment at 350 °C, the sheet resistance of the AgNP/PIB-POE-PIB/GO-4% hybrid with a 20:20:1 weight ratio was more than three orders of magnitude higher than that of the hybrids with 5:5:1 and 10:10:1 weight ratios (varying from 1.2×10^{2} to 9.6×10^{-1} Ω/sq). A hybrid film with sheet resistance as low as 5.2×10^{-2} Ω/sq could be prepared by controlling the heat-treated at 350 °C and by using AgNP/PIB-POE-PIB/GO-50% in a weight ratio of 20:20:1. The degree of difference depended on the AgNP content and dispersion of AgNPs with different GO oxygen contents. In contrast to the AgNP/PIB-POE-PIB/GO hybrids, the hybrid film containing no GO support (*i.e.*, AgNP/PIB-POE-PIB, weight ratio = 1:1) afforded a sheet resistance of 1.8×10^{-1} Ω/sq. This variation illustrates the advantage of using melted AgNPs for effective conducting fillers to improve the conductivity of these hybrid materials. Overall, excellent conductivity was achieved due to the effects of the melting behavior of silver.

Conclusions

We successfully developed novel nanohybrid surfactants to improve the dispersion of silver nanoparticles (AgNPs) and prepared highly conductive hybrid films. These novel organic/inorganic nanohybrid dispersants supported AgNPs in the *in situ* reduction of silver nitrate, employing DMF as a reducing agent in a water/DMF cosolvent system. Through a simple coating and heating process at 300 °C, silver aggregation and the formation of melting silver connections with silver-coated glass films were observed. On further increasing the temperature to 350 °C, the surface resistance decreased to 5.2×10^{-2} Ω/sq through the interconnected silver melt network structures. The resulting films were then employed to demonstrate their potential for use as nanoconductors in electronic devices.

Acknowledgments

We acknowledge financial support from the Aim for the Top University Plan of the National Taiwan University of Science and Technology and the Ministry of Science and Technology (MOST 103-2221-E-011-167- and MOST 104-2221-E-011-155-) of Taiwan.

Notes and references

1. K. S. Novoselov, A. K. Geim, S. V. Morozov, D. Jiang, Y. Zhang, S. V. Dubonos, I. V. Grigorieva and A. A. Firsov, *Science*, 2004, 306, 666–669.
2. K. S. Novoselov, A. K. Geim, S. V. Morozov, D. Jiang, M. I. Katsnelson, I. V. Grigorieva, S. V. Dubonos and A. A. Firsov, *Nature*, 2005, 438, 197–200.
3. Y. T. Weng and N. L. Wu, *J. Power Sources*, 2013, 238, 69–73.
4. H. W. Tien, Y. L. Huang, S. Y. Yang, J. Y. Wang and C. C. M. Ma, *Carbon*, 2011, 49, 1550–1560.
5. S. T. Hsiao, C. C. M. Ma, H. W. Tien, W. H. Liao, Y. S. Wang, S. M. Li and Y. C. Huang, *Carbon*, 2013, 60, 57–66.
6. X. Pu, H. B. Zhang, X. Li, C. Gui and Z. Z. Yu, *RSC Adv.*, 2014, 4, 15297–15303.
7. L. Liu, X. M. Bian, J. Tang, H. Xu, Z. L. Hou and W. L. Song, *RSC Adv.*, 2015, 5, 75239–75247.
8. M. C. Hsiao, C. C. M. Ma, J. C. Chiang, K. K. Ho, T. Y. Chou, X. Xie, C. H. Tsai, L. H. Chang and C. K. Hsieh, *Nanoscale*, 2013, 5, 5863–5871.
9. A. Choudhury, *RSC Adv.*, 2014, 4, 8856–8866.
10. W. Ye, L. Zhang and C. Li, *RSC Adv.*, 2015, 5, 25450–25456.
11. B. Yuan, L. Song, K. M. Liew and Y. Hu, *RSC Adv.*, 2015, 5, 41307–41316.
12. N. H. Yang, Y. S. Wu, J. Chou, H. C. Wu and N. L. Wu, *J. Power Sources*, 2015, 296, 314–317.
13. J. H. Seol, I. Jo, A. L. Moore, L. Lindsay, Z. H. Aitken, M. T. Pettes, X. Li, Z. Yao, R. Huang, D. Broido, N. Mingo, R. S. Ruoff and L. Shi, *Science*, 2010, 328, 213–216.
14. H. Yao, T. C. Huang and H. J. Sue, *RSC Adv.*, 2014, 4, 61823–61830.
15. P. T. K. Loan, W. Zhang, C. T. Lin, K. H. Wei, L. J. Li and C. H. Chen, *Adv. Mater.*, 2014, 26, 4838–4844.
16. N. Hong, Y. Pan, J. Zhan, B. Wang, K. Zhou, L. Song and Y. Hu, *RSC Adv.*, 2013, 3, 16440–16448.
17. B. Yu, X. Wang, X. Qian, W. Xing, H. Yang, L. Ma, Y. Lin, S. Jiang, L. Song, Y. Hu and S. Lo, *RSC Adv.*, 2014, 4, 31782–31794.
18. D. V. Thanh, L. J. Li, C. W. Chu, P. J. Yen, K. H. Wei, *RSC Adv.*, 2014, 4, 6946–6949.
19. B. Yu, Y. Shi, B. Yuan, L. Liu, H. Yang, Q. Tai, S. Lo, L. Song and Y. Hu, *RSC Adv.*, 2015, 5, 13502–13506.
20. T. M. Swager, *ACS Macro Lett.*, 2012, 1, 3−5.
21. P. T. C. Lee, C .W. Chiu, L. Y. Chang, P. Y. Chou, T. M. Lee, T. Y. Chang, M. T. Wu, W. Y. Cheng, S. W. Kuo and J. J. Lin, *ACS Applied Materials & Interfaces*, 2014, 6, 14345−14352.
22. C. W. Chiu, C. A. Lin and P. D. Hong, *J. Polym. Res.*, 2011, 18, 367–372.
23. N. Gao, T. Yang, T. Liu, Y. Zou and J. Jiang, *RSC Adv.*, 2015, 5, 55801–55807.
24. I. L. Gunsolus, M. P. S. Mousavi, K. Hussein, P. Bühlmann and C. L. Haynes, *Environ. Sci. Technol.*, 2015, 49, 8078–8086.
25. A. Kayet, D. Datta, G. Kumar, A. S. Ghosh and T. Pathak, *RSC Adv.*, 2014, 4, 63036–63038.
26. M. Vaseem, K. M. Lee, A. R. Hong and Y. B. Hahn, *ACS Appl. Mater. Interfaces*, 2012, 4, 3300–3307.
27. S. Anandhakumar, M. Sasidharan, C. W. Tsao and A. M. Raichur, *ACS Appl. Mater. Interfaces*, 2014, 6, 3275–3281.
28. J. C. Trefry, J. L. Monahan, K. M. Weaver, A. J. Meyerhoefer, M. M. Markopolous, Z. S. Arnold, D. P. Wooley and I. E. Pavel, *J. Am. Chem. Soc.*, 2010, 132, 10970–10972.
29. T. Öhlund, A. Schuppert, B. Andres, H. Andersson, S. Forsberg, W. Schmidt, H. E. Nilsson, M. Andersson, R. Zhang and H. Olin, *RSC Adv.*, 2015, 5, 64841–64849.

RSC Advances Accepted Manuscript

30. L. Ke, S. C. Lai, H. Liu, C. K. N. Peh, B. Wang and J. H. Teng, *ACS Appl. Mater. Interfaces*, 2012, 4, 1247–1253.
31. J. R. Greer and R. A. Street, *Acta Materialia*, 2007, 55, 6345–6349.
32. L. Tzounis, R. Contreras-Caceres, L. Schellkopf, D. Jehnichen, D. Fischer, C. Cai, P. Uhlmann and M. Stamm, *RSC Adv.*, 2014, 4, 17846–17855.
33. Y. Xuan, H. Duan and Q. Li, *RSC Adv.*, 2014, 4, 16206–16213.
34. H. Liu, J. Bai, C. Li, W. Xu, W. Sun, T. Xu, Y. Huang and H. Li, *RSC Adv.*, 2014, 4, 3195–3200.
35. Q. Zhang, C. Zhou and A. Huang, *RSC Adv.*, 2015, 5, 91056–91061.
36. A. Patole and G. Lubineau, *Carbon*, 2015, 81, 720–730.
37. B. M. Amoli, J. Trinidad, A. Hu, Y. N. Zhou and B. Zhao, *J Mater Sci: Mater Electron*, 2015, 26, 590–600.
38. C. W. Chiu, G. B. Ou, Y. H. Tsai and J. J. Lin, *Nanotechnology*, 2015, 26, 465702.
39. C. W. Chiu, P. D. Hong and J. J. Lin, *Langmuir*, 2011, 27, 11690–11696.
40. Y. R. Chen, K. F. Chiu, H. C. Lin, C. L. Chen, C. Y. Hsieh, C. B. Tsai and B. T. T. Chu, *Solid State Sci.*, 2014, 37, 80–85.
41. Y. R. Chen, K. F. Chiu, H. C. Lin, C. Y. Hsieh, C. B. Tsai and B. T. T. Chu, *Mater. Sci. Eng. B*, 2014, 190, 59–65.
42. W. C. Chen, C. Y. Hsieh, Y. T. Weng, F. S. Li, H. C. Wu and N. L. Wu, *J. Appl. Electrochem.*, 2014, 44, 1171–1177.

RSC Advances Accepted Manuscript

This journal is © The Royal Society of Chemistry 20xx

Table of Contents

Facile preparation of highly electrically conductive films of silver nanoparticles finely dispersed in polyisobutylene-*b*-poly(oxyethylene)-*b*-polyisobutylene triblock copolymers and graphene oxide hybrid surfactants

Chih-Wei Chiu* and Gang-Bo Ou

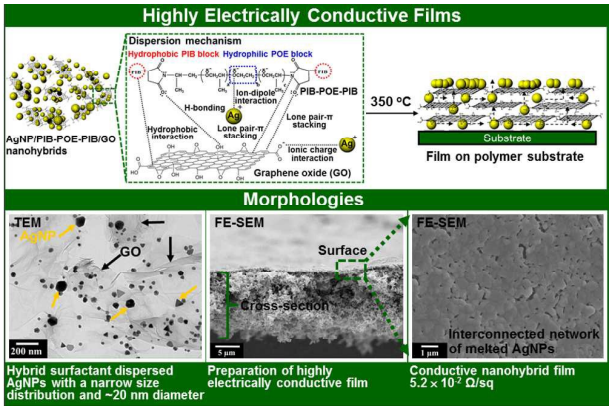

The melted morphologies revealed that the AgNPs possessed mobility, and melted on the film surface, giving a high electrical conductivity of 5.2×10^{-2} Ω/sq when heat-treated at 350 °C.

RSC Advances Accepted Manuscript